JOURNAL OF GEOPHYSICAL RESEARCH, VOL. 113, D14108, doi:10.1029/2007JD009392, 2008

Attempt to identify sources of atmospheric methane and carbon dioxide concentrations found in in situ aircraft measurements over Southern Australia

Ryu Saito,[1] Jörg M. Hacker,[2] Gen Inoue,[3] and Tatsuya Yokota[1]

Received 16 September 2007; revised 23 December 2007; accepted 19 March 2008; published 17 July 2008.

[1] Identifying the sources and sinks of methane and carbon dioxide is important for understanding processes within the Earth's climate system. This paper attempts to use back trajectories to identify sources of atmospheric methane and carbon dioxide as measured by high resolution in situ gas analyzers during aircraft ascents and descents in Southern Australia. Results from the back trajectory analysis were confirmed by also performing a forward trajectory analysis on some of the data. The in situ aircraft measurements were part of a joint Japanese-Australia field campaign in March and April 2007 near Adelaide, South Australia. The vertical profiles showed considerable variation in methane and carbon dioxide content above the planetary boundary layer. We used back trajectories based on an atmospheric transport model to derive the origin of the air masses which enabled speculation about sources of the gases. We were thus able to identify emission from the volcanoes on Réunion Island in the Indian Ocean and the seafloor hydrothermal activity in the Southeast Indian Ridge, confirming speculations published earlier by other research teams.

Citation: Saito, R., J. M. Hacker, G. Inoue, and T. Yokota (2008), Attempt to identify sources of atmospheric methane and carbon dioxide concentrations found in in situ aircraft measurements over Southern Australia, *J. Geophys. Res.*, *113*, D14108, doi:10.1029/2007JD009392.

1. Introduction

[2] Determining the location and strength of sources and sinks of greenhouse-active gases is important to study Global Warming and, more generally, the Earth System Sciences such as climate change, biogeochemical cycles, the atmospheric heat energy budget, atmosphere-ocean interaction. The combination of back trajectories with measurements of vertical profiles of the atmospheric methane (CH_4) and carbon dioxide (CO_2) concentrations augmented and confirmed by a suitable forward trajectory analysis and/or chemical GCM simulation can be regarded as a valuable tool to identify sources of these gases and how the concentrations might change during the transport process. Therefore atmospheric mixing ratios observed from aircraft sampling missions or from fixed monitoring sites have been also analyzed by using back trajectory calculations to help interpret their data as a regular occurrence [e.g., *Newell and Evans*, 2000; *Zhang et al.*, 2007; *Oshima et al.*, 2004; *Mak et al.*, 2000; *Koike et al.*, 2003; *Yamanouchi et al.*, 2005].

[3] In situ measurements of the atmospheric CH_4 and CO_2 have been conducted worldwide. For example, since the mid-1990s, passenger aircraft carried instrumented cargo containers along regular air routes, especially over the Northern hemisphere. Typical projects were the Measurement of OZone and water vapor by AIrbus in-service airCraft (MOZAIC: Germany) [*Suhre et al.*, 1997; *Sauvage et al.*, 2007], the Integration of routine Aircraft measurements into a Global Observing System (IAGOS: Germany), and the Civil Aircraft for the Regular Investigation of the atmosphere Based on an Instrument Container (CARIBIC: France) [*Zahn et al.*, 2002]. These flight mainly covered air routes between Europe and North/South America, Asia and Africa, while the Comprehensive Observation Network for TRace gases by AIrLiner (CONTRAIL: Japan) covers East Asia from North America, Europe, and Australia. Several more local airborne measurement campaigns were also sporadically carried out around the world, even in isolated areas such as Siberia [*Tohjima et al.*, 1993, 1996] and the Amazon rain forest [*Miller et al.*, 2007]. On the ground, in situ devices such as instrumented floats were deployed on all oceans in the context of the Global Ocean Observing System (GOOS) are. Observations were also taken from ships of opportunity.

[4] Based on these in situ measurements, overall vertical and horizontal distributions of these gases have been developed and linked to simulations of processes, such as source and sink budget flux model [*Jagovkina et al.*, 2004; *Robert et al.*, 2002], and the atmospheric transport model [*Zeng et al.*, 2003a]. Meanwhile, *Kasai et al.*

[1]Center for Global Environmental Research, National Institute for Environmental Studies, Tsukuba, Ibaraki, Japan.
[2]Airborne Research Australia, Flinders University, South Australia, Australia.
[3]Graduate School of Environmental Studies, Nagoya University, Nagoya, Aichi, Japan.

0148-0227/08/2007JD009392$09.00

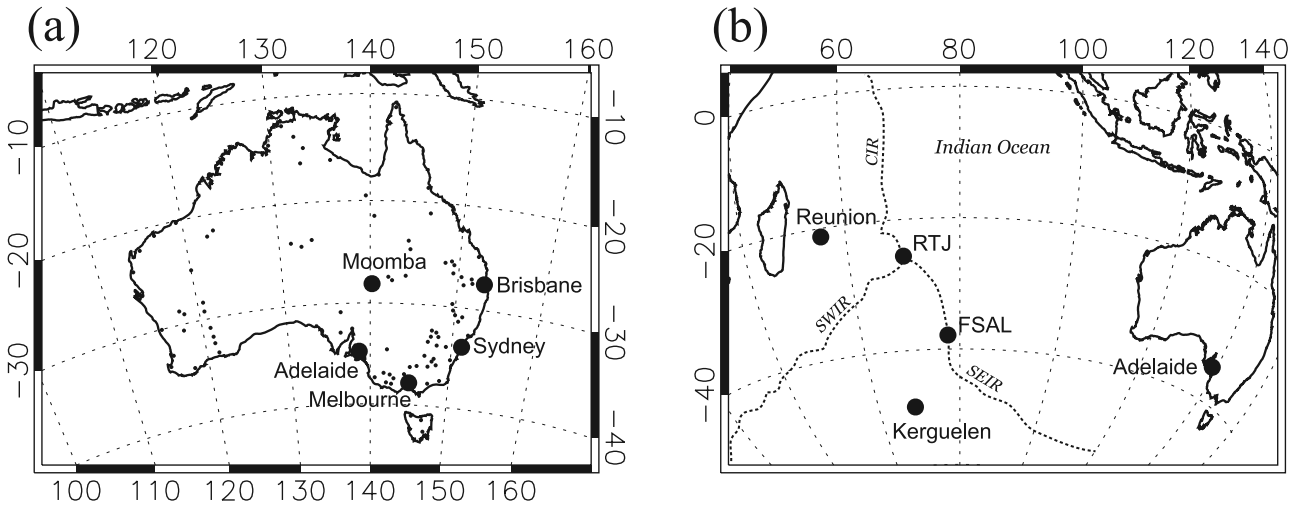

Figure 1. Positions of sampling sites and other locations referred to in the text. (a) Major cities in southeastern Australia and gas fuel stations marked as small dots which are relevant to anthropogenic sources of CH_4 and CO_2. (b) Volcanic islands and ridges in the Indian Ocean relevant for natural sources.

[2005] compared measurements using a ground-based Fourier Transform Spectrometer (FTS) with total column measurements combined with a trajectory model. Furthermore, researchers are planning to validate direct FTS-measurements of the total column content of CH_4 and CO_2 with retrieved total column values from satellites instruments, e.g., existing the SCanning Imaging Absorption SpectroMeter for Atmospheric CHartographY (SCIAMACHY) [*Bovensmanna et al.*, 1999], and the Greenhouse gases Observing SATellite (GOSAT) and the Orbiting Carbon Observatory (OCO) [*Crisp et al.*, 2004] currently under development.

[5] However, there are two problems with these comparisons and validations. First, there are very few in situ measurements available over the oceans, especially the South Indian Ocean. Unlike in the Pacific Ocean which has some island-based scientific observing stations (e.g., Hawaii, Galapagos, and Tahiti), the Southern Indian Ocean is far from the continents and only few air shipping routes cross it. The only islands offering scientific facilities are near the edge of the Indian Ocean: La Réunion (21.1°S, 55.5°E) and the Kerguelen Islands (Figure 1b). It is therefore difficult to establish continuous or more intense observations of the natural sources located there, such as mud volcanoes [*Kopf*, 2003; *Svensen et al.*, 2004] and the seafloor hydrothermal activity in the Indian ridges on the seafloor [*Gamo et al.*, 1996; *Kelley and Früh-Green*, 1999]. Second, direct measurements and other results using FTS technology or models have so far mainly been compared with total column estimates, rather than with vertical profiles, because retrieved total column observations are generally more precise than retrieved vertical profile estimates. Total column estimates cannot really resolve the vertical distribution of the gases and thus are not reliable in determining individual sources. In contrast, vertical profile measurements of the gas concentrations can be combined with back air mass trajectories at individual layers of the vertical profiles to reveal their transport process and speculate on their sources [e.g., *Newell and Evans*, 2000; *Zhang et al.*, 2007; *Oshima et al.*, 2004; *Mak et al.*, 2000; *Koike et al.*, 2003; *Yamanouchi et al.*, 2005]. In the same sense, we used this technique to interpret the measured vertical profiles from the field campaign. Provided an air mass has mainly been transported above the planetary boundary layer (PBL) and there are no significant anthropogenic sources, this technique can be used over long distances and from regions where sparse or no source information is available. To confirm the findings from the back trajectory analyses and our speculations about the sources, a forward trajectory-type model was used which includes vertical transport process that affect the air mass and concentrations over the period of the back trajectory analysis.

[6] The observational site was located near Adelaide, South Australia, which is normally downwind of the South Indian Ocean (Figures 1a and 1b). We guessed that, as there are very few anthropogenic sources of CH_4 and CO_2 between the Indian Ocean and Southern Australia, the air arriving over Southern Australia should often have been affected by natural sources.

2. Methods

[7] Instrumentation for the measurements of CO_2, CH_4, particle number density and standard meteorological parameters (i.e., temperature, pressure, humidity, and wind) was flown on 22, 25, and 26 March, and 5 April 2007 on the Australian research aircraft ECODimona HK36TTC of the Airborne Research Australia (ARA) [*Hacker*, 1996]. The operations base for all flight activities was Parafield Airport just north of Adelaide (34.8°S, 138.6°E). All flights were conducted within a radius of 40 km around Adelaide and consisted of one descending and one ascending profile from the surface to approximately 5500 m. The flight duration was typically 2 h: 4:15 to 5:15 UTC on 22 March 2:00 to 3:50 UTC on 25 March 6:00 to 7:55 UTC on 26 March and 4:35 to 6:05 UTC on 5 April. All observing instruments in the aircraft were operated automatically during the flights.

[8] Methane was measured using a SnO_2-based sensor [*Suto and Inoue*, 2004; *Madhusudhana Reddy and Chandorkara*, 1999], and carbon dioxide was measured using an infrared

gas analyzer Li-COR LI-820. These instruments were periodically calibrated in flight by switching the gas inlet from outside air to the two different known standards of 1.746 ppm and 2.018 ppm for CH_4 and 382.6 ppm and 402.0 ppm for CO_2, based on the National Institute for Environmental Studies (NIES) standard gas scale. Each standard was supplied to the instruments for 4 min every half an hour. The particle number density was measured for the sizes 0.5, 1.0, and 3.0 μm, using a laser particle counter (LPC: Lighthouse Handheld-5016). The meteorological parameters (air temperature, dew point, wind speed, wind direction, and pressure) were measured by the aircraft's standard instrumentation package.

[9] Back trajectory analyses were performed using the METEX (METeorological data EXplorer: http://db.cger.nies.go.jp/metex/), developed by Zeng [*Zeng et al.*, 2003a, 2003b]. Synoptic data for the METEX was provided by the European Centre for Medium-Range Weather Forecasts (ECMWF). As the lifetimes of middle-upper tropospheric CH_4 and CO_2 are relatively long ($\gg$10 d) [*Brasseur et al.*, 1999], 10-d back trajectories were calculated for the air masses.

[10] As a dispersion model is not included in the METEX, it will not be able to asses vertical mixing processes related to turbulent mixing, such as convective processes, and vertical diffusion. Such processes can change the concentration of the gases in question considerably and prevent a meaningful identification of their. To assess these processes, we used the NOAA ARL HYSPLIT model (National Oceanic and Atmospheric Administration - Air Resources Laboratory - HYbrid Single-Particle Lagrangian Integrated Trajectory [*Draxler*, 1992]: http://www.arl.noaa.gov/ready/hysplit4.html) to simulate one of the observed cases.

3. Results and Discussion

[11] The vertical profiles of the concentrations of atmospheric CH_4 and CO_2 for the four flights as shown in Figure 2 depict marked differences from flight to flight, as well as for individual altitudes within a single flight. On 22 March, the aircraft reached an altitude of 4 km. The data are shown in Figure 2a and indicates a much higher concentration of CO_2 than for any of the other days, in particular for the CO_2 concentration below $\sim$1.3 km which is more than 3 ppm above the value for the remaining days. The sharp decrease of the CO_2 concentration (left-most column of Figure 2) at the top of the PBL is matched by a drop in particle number density (right-most column in Figure 2), as well as a weak temperature inversion (third column in Figure 2). Data from the flight on 25 March is shown in Figure 2b up to 6 km of altitude. The data gap between 4 km and 5 km is caused by the calibration procedure, when the system temporarily switched its gas inlet to the gas calibration standard, as described above. However, for CO_2 it was possible to use a secondary, less accurate, CO_2 instrument for this altitude range. As can be seen, trends in the CO_2 and CH_4 profiles were similar with a maximum value around 3 km and lowest values below $\sim$1.8 km. The vertical extend of the PBL can be seen in the dew point and temperature profiles with a temperature inversion at $\sim$1.5 km. Above the inversion, the dew point dropped sharply, as do the particle number concentrations. The profiles of temperature and dew point on 26 March were similar (see Figure 2c), except that humidity was higher at higher altitudes than on 25 March. The particle number densities showed a more pronounced minimum above the inversion. In the PBL, the CO_2 concentration had increased by more than 1.5 ppm above the values on the previous day, while the CH_4 concentration above 4 km had increased. Therefore unlike on the previous day, the vertical trend of CO_2 was not similar to that of CH_4. On 5 April (Figure 2d), both the CO_2 and CH_4 profiles were recognized as being almost constant vertically, except that the CO_2 concentration in the PBL ($\sim$1.2 km) was the smallest one observed during the measurement campaign ($\sim$378.5 ppm).

[12] Generally, there should be a good correlation between the vertical profiles of CH_4 and CO_2 one (as is the case for 25 March and 5 April), and both profiles should have an approximately homogeneous vertical distribution in the troposphere. We hypothesize that the inhomogeneous vertical profiles on each day, as well as the weak correlation between the CO_2 and CH_4 profiles on 22 and 26 March are a result of air masses of different origin being advected at different altitude over Southern Australia. Differences in the shape of the profiles, as well as the day-to-day concentrations can be affected dramatically by anthropogenic influence and natural processes such as volcanic eruptions, forest fires, changes in permafrost, and wetland-related biological activities to which the air masses are subjected during their transport from the source region to the point of the measurement. Using an atmospheric transport model, we attempt to estimate the influences which led to the observed profiles.

[13] Figure 3 shows the trajectories of the air masses for the four flight days, where the colors encode the altitudes and the panels (from the top) represent the day of arrival of the air masses over Adelaide. Depicted are trajectories for a 10-d period before each of the flight days. The air mass reaching Adelaide on 22 March at 4 a.m. UTC (Figure 3a) circled around Eastern Australia anticlockwise at all altitudes. By contrast, the tracks for the other days, (Figure 3b) 25 March, (Figure 3c) 26 March, (Figure 3d) 5 April, have their origins over the ocean to the Southwest or West of Australia, that is, the Southwest Indian Ocean, the Southern Ocean, and the South Atlantic Ocean, depending on altitude. The trajectories starting from different altitudes at Adelaide for 25 March (Figure 3b) in the green line (4 km altitude) and the blue line (3 km altitude) are similar to those for 26 March (Figure 3c). However, the trajectories depicted in the red line (5 km altitude) show that the origin of the air was in Southern South America, as is the case for 5 April (Figure 3d). The air in the PBL over Adelaide (the brown lines) originated from oceanic regions to the South on 25 March and 5 April, but had arrived over Adelaide indirectly via the inland of Australia on 22 March and 26 March.

[14] Inspecting the horizontal plan view of the trajectories in Figure 3, some of the features in the vertical profiles from the different days can be explained. For instance, the profiles on 22 March (Figure 2a) which are rather different from all other profilers can be explained by the different trajectories for the 10-d period leading to that date (in Figure 3a) when compared to the other trajectories. As the air arriving over Adelaide on 22 March had spent much

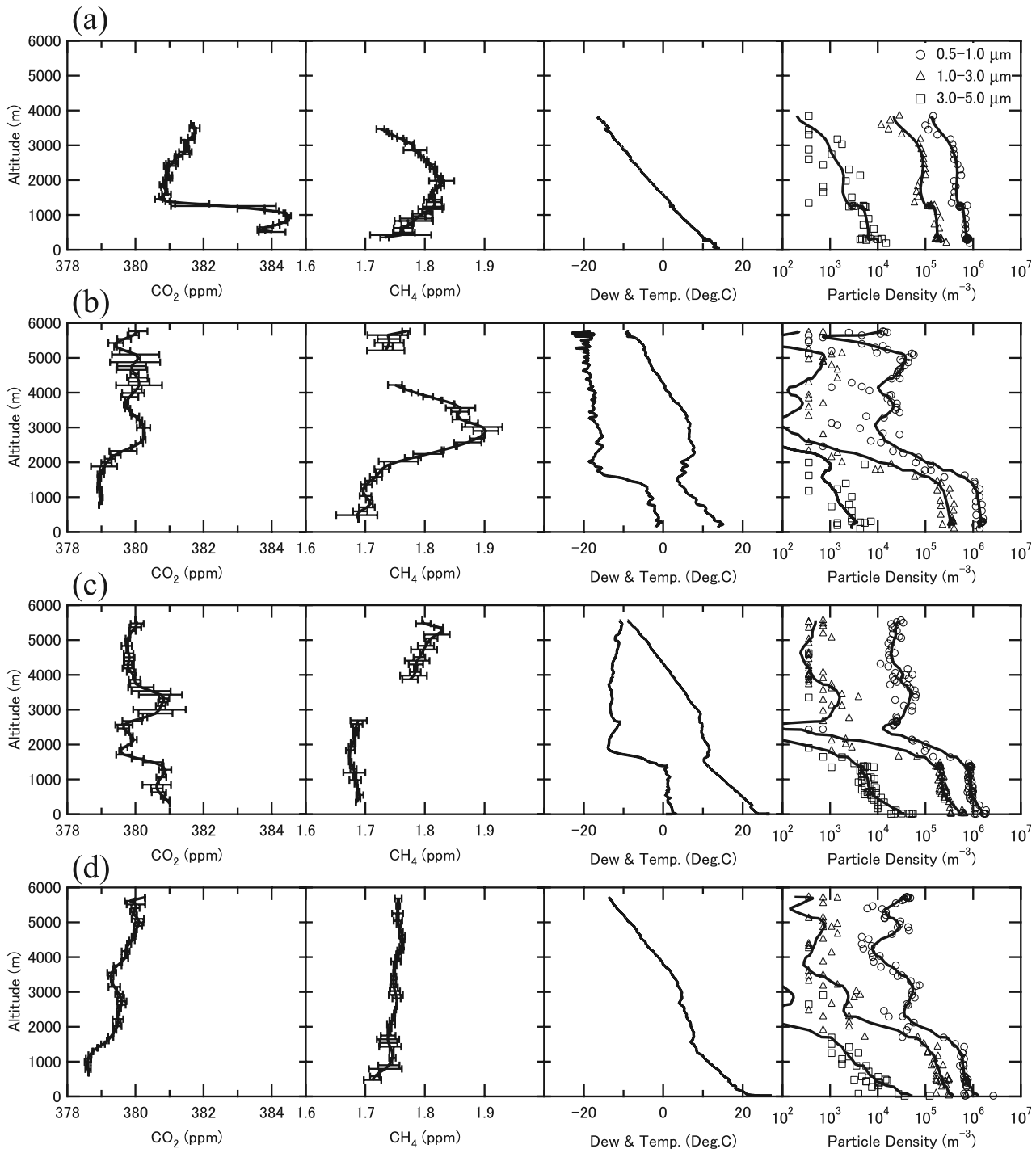

Figure 2. Vertical profiles of (from left to right) CO_2, CH_4, air temperature and dew point, and particle number densities from the airborne in situ measurements. From top to bottom, data are shown for (a) 22 March, (b) 25 March, (c) 26 March, and (d) 5 April. CO_2, CH_4, and weather parameters are averages from the ascent and descent. The horizontal bars show the standard deviation and the mean. Gaps in the CO_2 and CH_4 data are caused by the calibration procedure (see text). No dew point data were available on 22 March and 5 April. The particle number density is plotted by the marks and its smooth lines.

more time over continental Australia than that for the other days, a comparatively high CO_2 concentration can be observed in the PBL, as well as in the higher levels of the troposphere. A similar, yet less strong effect can be seen in the particle number densities. Another example are the trajectories originating off the coast of Eastern Madagascar for the 10 d leading to 25 and 26 March (Figures 3b and 3c), on which days the CH_4 concentration was observed to be higher.

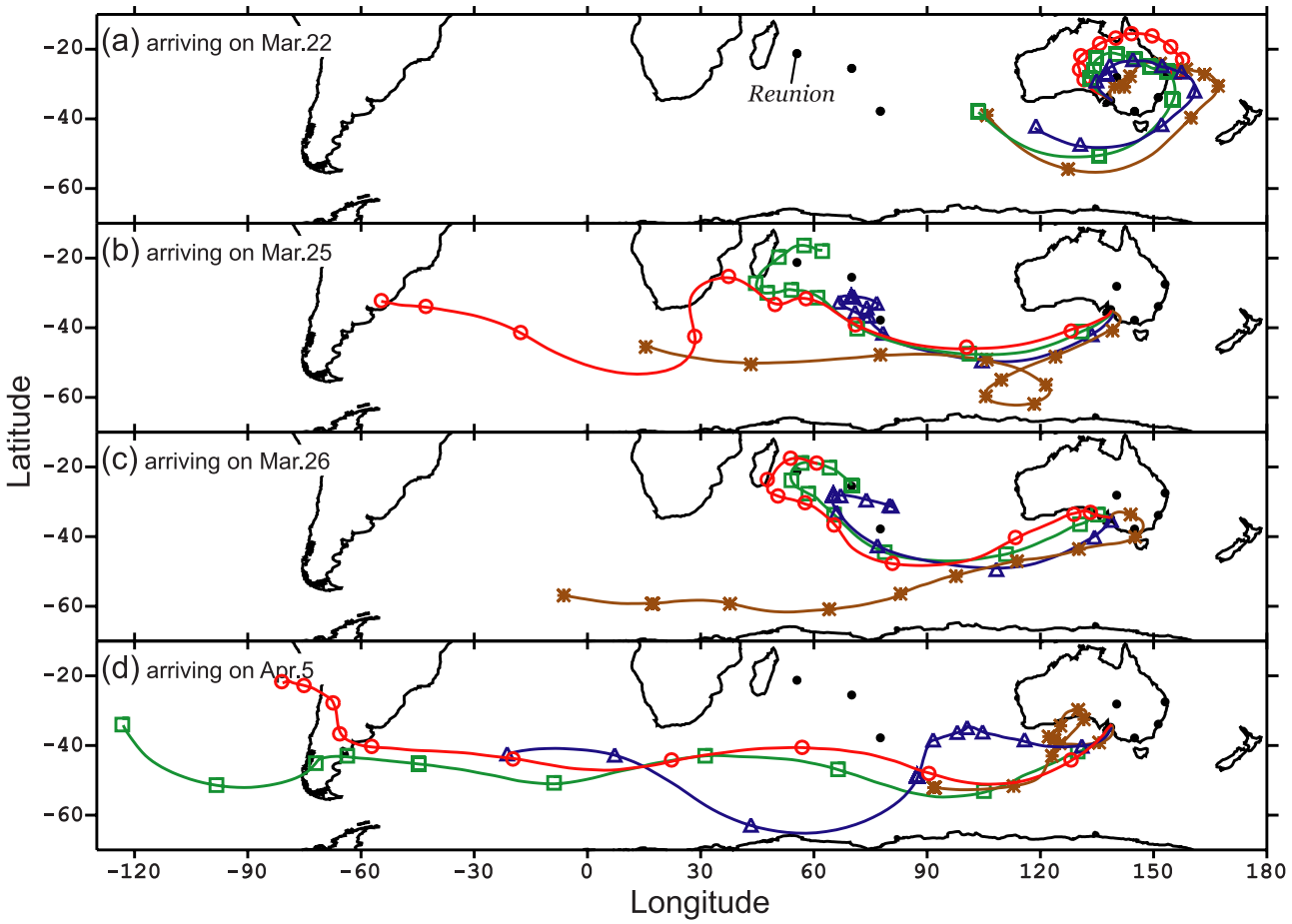

Figure 3. Back trajectories over 10-d periods prior to each of the four flight dates. Figures 3a, 3b, 3c, and 3d show the trajectories for air mass arriving on 22 March at 4 a.m. UTC, 25 March at 3 a.m., 26 March at 7 a.m., and 5 April at 6 a.m., respectively. Red lines are trajectories for 5 km; green lines for 4 km; blue lines for 3 km; and brown lines for 1 km altitude over Adelaide. Symbols are plotted every 24 h.

[15] To investigate the variations in the profiles further, it is also useful to study the altitudes at which the air mass was transported over the 10-d periods. Figure 4 shows plots of the altitude of the transport versus the distance along the trajectory for each of the 10-d back trajectories. For 22 March (Figure 4a), the two lowest trajectories (marked by asterisk and triangles) reached a minimal height (<~2.2 km) on 19 March near the Moomba oil and gas fields (see Figure 1a), whereas they had been transported at altitudes above 4 km off Southern Australia and over Eastern Australia during the 12 to 15 March period. In contrast to most other trajectories, the one for the air that arrived at 5 km altitude over Adelaide on 25 March (Figure 4b, circles) remained most of the 10-d period above 4 km originating from over the East coast of South America. For the same day, the trajectories arriving at 4 km or below have their origins near the coast of Eastern Madagascar (Figures 4b and 3b). Likewise, all the trajectories for 26 March (Figure 4c) originate at lower altitudes. In particular, it can be seen that the air arriving on that day at the highest level (Figure 4c, circles) had spent several days (16 to 18 March) near the sea surface before it crossed over Réunion Island (see Figure 1b). After that, it was lifted and transported toward Southern Australia.

[16] The above trajectory analysis allows speculation about sources of anthropogenic or natural origin affecting the observed vertical profiles of the concentrations of CH_4 and CO_2. As is well known anthropogenic sources predominate in urban and industrial areas [*Brasseur et al.*, 1999]. Therefore we can assume that the comparatively high CO_2 and to a lesser degree CH_4 concentrations observed on 22 March is at least partly a result of the air mass having been transported for long distances at low level over Eastern Australia. This is in line with results from the Australian emission model of *Wang and Bentley* [2002]. For instance, the back trajectory for 22 March (Figures 3a and 4a) crossed to lower layers near Brisbane on 18 March, and the trajectory for 26 March (Figures 3c and 4c) crossed the coast near Melbourne on 24 to 25 March. This allowed the air to pick up higher levels of CO_2 in the PBL (Figures 2a and 2c). Another example of this process might be manifested by the higher concentrations of not only CO_2 but also CH_4 when the trajectories pass close to the Moomba oil and gas fields (see Figure 1). Taking

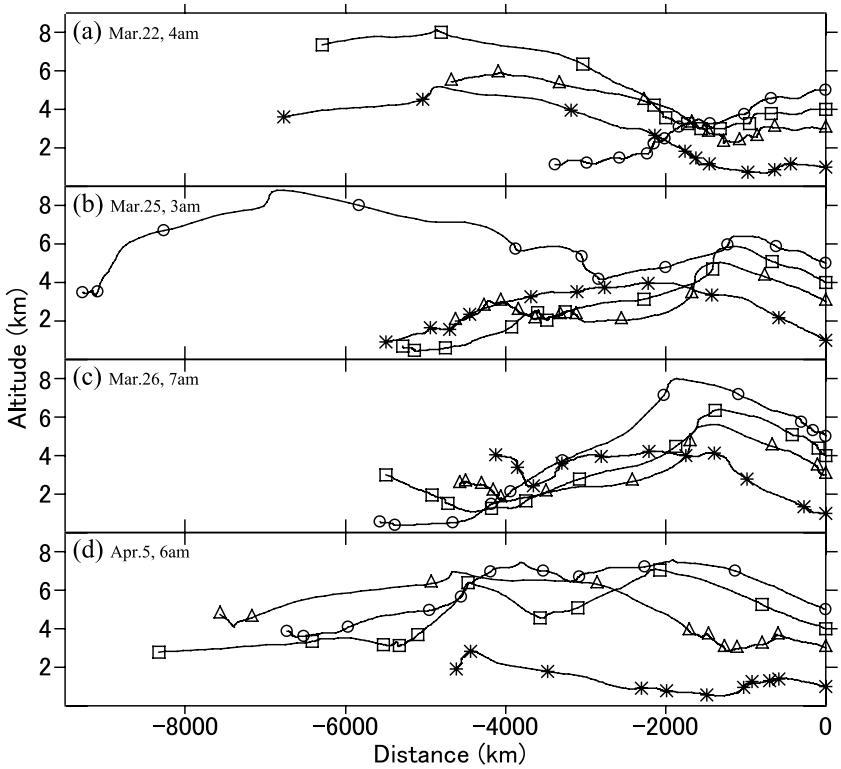

Figure 4. Altitudes of the back trajectories versus distance from Adelaide along the trajectories for the four flights. (a) 22 March at 4 a.m. UTC, (b) 25 March at 3 a.m., (c) 26 March at 7 a.m., (d) 5 April at 6 a.m. Symbols are plotted every 24 h. Asterisks, triangles, squares and circles mark trajectories arriving at one km, three km, four km and five km overhead Adelaide, respectively.

this concept a step further, one can speculate furthermore that more CH_4 and CO_2 might be added to the air by the fact that major trunk lines of Australian's oil and gas pipeline network is located in the Southeast corner of the country (from the Pipeline Publication Australia), where the air arriving over Adelaide on 22 March had spent considerable time at lower altitudes.

[17] Apart from anthropogenic sources as discussed above, natural sources can also contribute substantially to the concentrations of CH_4 and CO_2. For instance, volcanic eruptions can add a large amount of these gases to the atmosphere and as such can have strong effects on the climate [*Kopf*, 2003]. It can be hypothesized in this sense that the high CH_4 (∼1.8 ppm) and CO_2 (∼380 ppm) concentrations found around 4 km on 25 and 26 March (Figures 2b and 2c) have their origin in air that crossed over Réunion Island (green lines in Figures 3b and 3c) several days beforehand, where the Piton de la Fournaise volcano (∼2600 m AMSL) has been active, exhibiting activity levels similar to those of the most active volcanic hot spots of the type found on the Hawaiian Islands [*Lopes*, 2005]. Indeed, the Piton de la Fournaise erupted violently on 1 April 2007 after ongoing lower intensity eruptive activity since 12 February 2007, as reported by the Observatoire Volcanologique du Piton de La Fournaise (OVPF). During these times, the volcano released large quantities of volcanic gases: H_2O, SO_2, CO_2, CH_4, H_2S, and others into the atmosphere.

[18] The air mass over Réunion Island during 16 to 17 March (Figure 4b) and 18 to 19 (Figure 4c) must have contained enough volcanic gases to increase the transported CH_4 and CO_2 at around 4 km near Adelaide on 25 and 26 March. To confirm these sources, the HYSPLIT trajectory and dispersion model was used and the results are shown in Figure 5. Depicted are concentrations (an arbitrarily set to one unit source: e.g., ppm m^{-3}, kg m^{-3}, and mol m^{-3}) showing plumes extending to the west of Réunion Islands during 16 March (shaded colors in Figure 5). The air mass of this area rich in information of sources was calculated by 3-d forward trajectory starting from 16 March at the three altitudes (1.0, 1.5, and 2.0 km) on each of the five positions around Réunion Islands: (20°S, 54°E), (20°S, 56°E), (21°S, 55°E), (22°S, 56°E), and (22°S, 56°E). The air of the 10-d back trajectory from Adelaide on March 25 (the green line in Figure 5) has crossed and suffered from influence of the Réunion's events on 16 and 17 March, which would be the evidence in support of the air mass rich in CH_4 and CO_2. The air mass affected by the dispersion traveled in the direction of Adelaide.

[19] On the basis of the measurements and trends in the CO_2 and particle number density profiles at 3 km on 25 and 26 March (Figures 2b and 2c), it could be speculated that the CH_4 profile in the range of the missing data would have been similar to that of 25 March, because the air in that altitude band had been transported from another volcanic area around the French Southern and Antarctic Lands (FSAL), including Amsterdam (37.8°S, 77.6°E) and Saint

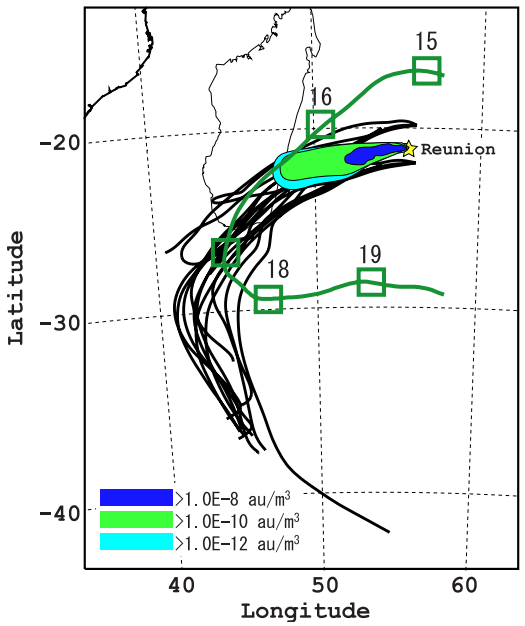

Figure 5. Concentrations integrated from 16 to 17 March and 3-d forward trajectories starting from 16 March around Réunion Island using the HYSPLIT dispersion and trajectory model, respectively. The green line and the 5 square symbols mark the dates of 15 to 19 March along the same back trajectory as shown (also in green) in Figure 3b. For more details, see text.

Paul Islands (38.7°S, 77.5°E), see Figures 1b, 3b and 3c. However, although these islands were formed by volcanic activity, the activity has since ceased. Hence the increased level of especially CH_4 (~1.9 ppm) around the 3 km level must have different origins.

[20] There are two other possible sources for CH_4 and CO_2 in these areas, the first one of these being hydrothermal activity on the seafloor. The Indian Ocean has the Central Indian Ridge (CIR), the Southeast Indian Ridge (SEIR), and the Southwest Indian Ridge (SWIR) which come together at the Rodriguez Triple Junction (RTJ) (25.5°S, 70.0°E) in Figure 1b. Some studies of the seafloor have been carried out around the RTJ and extraordinary hydrothermal plumes were found containing large amounts of CH_4 and Mn [*Gamo et al.*, 1996; *Kelley and Früh-Green*, 1999]. However, the studies of these ridges have not reached a point where it can be established if these plumes are larger or smaller than those emanating from similar ridges in the Pacific and Atlantic Ocean following *Sigurdsson et al.* [1999]. The only conclusion possible at this stage is that the plumes in this area might lead to an increase in the atmospheric CH_4 and CO_2.

[21] The second possible sources are emissions from mud volcanoes and cold seeps on the seafloor related to decomposing gas hydrates. A large number of mud volcanoes on the seafloor may contribute significantly to the oceanic methane pool [*Sauter et al.*, 2006], with 10^3–10^5 mud volcanoes believed to store 10^{10}–10^{12} m^3 of CH_4 (54–5400 Mt of carbon) in associated gas hydrates [*Milkov*, 2000]. These are estimated to release ~27 Mt methane a^{-1} to the ocean [*Milkov et al.*, 2003] on a worldwide basis. However, this amount is much smaller than the estimated 10^4 Gt of methane-carbon in gas hydrates. Therefore it can be assumed that CH_4 from oceanic sources only makes a small contribution of ~2.5% to the atmospheric CH_4 budgets [*Lelieveld et al.*, 1998]. On the other hand, CH_4 is distributed by plume currents rather than oxidized rapidly because of the rising bubble plumes [*Sauter et al.*, 2006]. Altogether, the CH_4 reaches the sea surface before it is being broken down by chemical reactions or microbes. This indicates that the concentrated CH_4 might exist in the lower levels of the marine atmosphere over areas of mud volcanoes and decomposing gas hydrates. An open question is whether such oceanic sources are significantly present in the SEIR. There are very few surveys of the seafloor hydrothermal activity in the Indian Ocean [*Sigurdsson et al.*, 1999], especially in the SEIR far from continents or islands. Therefore we suggest that the oceanic sources such as mud volcanoes can occur in the SEIR, as they do in the vicinity of other oceanic ridges, and affect air masses in such area.

[22] In this study, we have show that the inhomogeneous vertical profiles can at least partially be explained by the sources identified in the South Indian Ocean, an area which is nearly totally devoid of other observations. Such an analysis is essential for the development of numerical models of the processes involved. However, with the limited data available from this study, only a qualitative assessment of the sources and transport mechanisms was possible. A more quantitative assessment including the study of various scenarios and hypotheses require more high-resolution ground-based and aircraft-derived data, as well as data from existing satellites and satellites under development, coupled with a sophisticated numerical model.

4. Conclusions

[23] An atmospheric transport model was used to derive air mass trajectories of atmospheric CH_4 and CO_2 which influence vertical profiles of these gases over Southern Australia. Furthermore, anthropogenic and natural activities, were evaluated which influence the concentrations of these gases during the transport from the source regions to the point of measurement. We were able to find evidence that one of the natural sources is are volcanic plumes from the Piton de la Fournaise volcano on Réunion Island, with further contributions from mud volcanoes and seafloor hydrothermal activity in the Southeast Indian Ridge. The vertical profiles derived from the in situ aircraft measurements contributed not only to observing local phenomena such as fluxes from the surface, and comparing the total column concentration as measured by instruments such as an FTS, but also enable speculations about the contributions in the concentrations of the gases from sources in regions far away from the location of the measurements.

[24] **Acknowledgments.** We thank Y. Kojima, Y. Kanata, and T. Nakayama at Nagoya University for their support and kind encouragement. We thank M. Wilksch from Airborne Research Australia, and H. Suto from the Japan Aerospace Exploration Agency for support and assistance in using the methane instrumentation. We thank T. Matsunaga and J. Zeng from the National Institute for Environmental Studies for teaching us how to use the METEX. This research was supported by funds for the Special

Account for Petroleum and the More Sophisticated Structure of Demand and Supply of Energy from the Japanese Ministry of the Environment.

References

Bovensmanna, H., J. P. Burrowsa, M. Buchwitza, J. Frericka, S. Noëla, V. V. Rozanova, K. V. Chanceb, and A. P. H. Goedec (1999), SCIAMACHY: Mission objectives and measurement modes, *J. Atmos. Sci.*, *56*, 127–150.

Brasseur, G., J. J. Orlando, and G. S. Tyndall (Eds.) (1999), *Atmospheric Chemistry and Global Change (Topics in Environmental Chemistry)*, 672 pp., Oxford Univ. Press, New York.

Buchwitz, M., et al. (2005), Atmospheric methane and carbon dioxide from SCIAMACHY satellite data: Initial comparison with chemistry and transport models, *Atmos. Chem. Phys.*, *5*, 941–962.

Crisp, D., et al. (2004), The orbiting carbon observatory (OCO) mission, *Adv. Space Res.*, *34*, 700–709.

Draxler, R. R. (1992), Hybrid single-particle Lagrangian integrated trajectories (HY-SPLIT): Version 3.0 – User's guide and model description, *NOAA Tech. Memo. ERL ARL-195*, 26 pp. and Appendices.

Gamo, T. E., et al. (1996), Hydrothermal plumes at the Rodriguez triple junction, Indian ridge, *Earth. Planet. Sci. Lett.*, *142*, 261–270.

Hacker, J. M. (1996), ''Airborne Research Australia (ARA)'' - A new research aircraft facility on the Southern Hemisphere, in *Proceedings of the 2nd International Airborne Remote Sensing Conference and Exhibition: Technology, Measurement and Analysis (24–27 June 1996, San Francisco, Calif.)*, vol. 2, pp. 123–131.

Jagovkina, S. V., I. L. Karol, V. A. Zubov, V. E. Lagun, A. I. Reshetnikov, and E. V. Rozanov (2004), Methane fluxes in west Siberia: 3-D regional model simulation, *Earth Environ. Sci.*, *1*, 429–436.

Kasai, Y. J., A. Kagawa, N. Jones, A. Fujiwara, K. Seki, Y. Murayama, and F. Murcray (2005), Seasonal variations of CO and HCN in the troposphere measured by solar absorption spectroscopy over Poker Flat, Alaska, *Geophys. Res. Lett.*, *32*, L19812, doi:10.1029/2005GL022826.

Kelley, D. S., and G. L. Früh-Green (1999), Abiogenic Methane in deep-seated mid-ocean ridge environments: Insights from stable isotope analyses, *J. Geophys. Res.*, *104*, 10,439–10,460.

Koike, M., et al. (2003), Export of anthropogenic reactive nitrogen and sulfur compounds from the East Asia region in spring, *J. Geophys. Res.*, *108*(D20), 8789, doi:10.1029/2002JD003284.

Kopf, A. J. (2003), Global methane emission through mud volcanoes and its past and present impact on the Earth's climate, *Int. J. Earth Sci.*, *92*, 806–816, doi:10.1007/s00531-003-0341-z.

Lelieveld, J., P. J. Crutzen, and F. J. Dentener (1998), Changing concentration, lifetime and climate forcing of atmospheric methane, *Tellus B*, *50*, 128–150.

Lopes, R. (2005), *The Volcano Adventure Guide*, 362 pp., Cambridge Univ. Press, New York.

Madhusudhana Reddy, M. H., and A. N. Chandorkara (1999), E-beam deposited SnO_2, Pt–SnO_2 and Pd–SnO_2 thin films for LPG detection, *Thin Solid Films*, *349*, 260–265.

Mak, J. E., M. R. Manning, and D. C. Lowe (2000), Aircraft observations of $\delta^{13}C$ of atmospheric methane over the Pacific in August 1991 and 1993: Evidence of an enrichment in $^{13}CH_4$ in the Southern Hemisphere, *J. Geophys. Res.*, *105*, 1329–1335.

Milkov, A. V. (2000), Worldwide distribution of submarine mud volcanoes and associated gas hydrates, *Mar. Geol.*, *167*, 29–42.

Milkov, A. V., R. Sassen, T. V. Apanasovich, and F. G. Dadashev (2003), Global gas flux from mud volcanoes: A significant source of fossil methane in the atmosphere and the ocean, *Geophys. Res. Lett.*, *30*(2), 1037, doi:10.1029/2002GL016358.

Miller, J. B., et al. (2007), Airborne measurements indicate large methane emissions from the eastern Amazon basin, *Geophys. Res. Lett.*, *34*, L10809, doi:10.1029/2006GL029213.

Newell, R. E., and M. J. Evans (2000), Seasonal changes in pollutant transport to the North Pacific: The relative importance of Asian and European sources, *Geophys. Res. Lett.*, *27*, 2509–2512.

Oshima, N., et al. (2004), Asian chemical outflow to the Pacific in late spring observed during the PEACE-B aircraft mission, *J. Geophys. Res.*, *109*, D23S05, doi:10.1029/2004JD004976.

Robert, G. K., et al. (2002), Towards robust regional estimates of CO_2 sources and sinks using atmospheric transport models, *Nature*, *415*, 626–630.

Sauter, E. J., S. I. Muyakshin, J.-L. Charlou, M. Schlüter, A. Boetius, K. Jerosch, E. Damm, J.-P. Foucher, and M. Klages (2006), Methane discharge from a deep-sea submarine mud volcano into the upper water column by gas hydrate-coated methane bubbles, *Earth Planet. Sci. Lett.*, *243*, 354–365.

Sauvage, B., R. V. Martin, A. van Donkelaar, X. Liu, K. Chance, L. Jaegle, P. I. Palmer, S. Wu, and T.-M. Fu (2007), Remote sensed and in situ constraints on processes affecting tropical tropospheric ozone, *Atmos. Chem. Phys.*, *7*, 815–838.

Sigurdsson, H., B. Houghton, S. R. McNutt, H. Rymer, and J. Stix (Eds.) (1999), *Encyclopedia of Volcanoes*, 1456 pp., Elsevier, New York.

Suhre, K., J.-P. Cammas, P. Nedelec, R. Rosset, A. Marenco, and H. G. J. Smit (1997), Ozone rich transients in the upper equatorial Atlantic troposphere, *Nature*, *388*, 661–663.

Suto, H., and G. Inoue (2004), Development of atmospheric methane sensor based on tin-dioxide flammable detector, *Eos Trans. AGU*, *85*(47), Fall Meet. Suppl., Abstract A51C-0796.

Svensen, H., S. Planke, A. Malthe-Sørenssen, B. Jamtveit, R. Myklebust, T. R. Eidem, and S. S. Rey (2004), Release of methane from a volcanic basin as a mechanism for initial Eocene global warming, *Nature*, *429*, 542–545.

Tohjima, Y., H. Wakita, S. Maksyutov, T. Machida, G. Inoue, N. Vinnichenko, and V. Khattatov (1993), Distribution of tropospheric methane over Siberia in July, *J. Geophys. Res.*, *102*, 25,371–25,382.

Tohjima, Y., S. Maksyutov, T. Machida, and G. Inoue (1996), Airborne measurements of atmospheric methane over oil fields in western Siberia, *Geophys. Res. Lett.*, *23*, 1621–1624.

Wang, Y.-P., and S. T. Bentley (2002), Development of a spatially explicit inventory of methane emissions from Australia and its verification using atmospheric concentration data, *Atmos. Environ.*, *36*, 4965–4975.

Yamanouchi, T., et al. (2005), Arctic Study of Tropospheric Aerosol and Radiation (ASTAR) 2000: Arctic haze case study, *Tellus B*, *57*, 141–152.

Zahn, A., C. A. M. Brenninkmeijer, W. A. H. Asman, P. J. Crutzen, G. Heinrich, H. Fischer, J. W. M. Cuijpers, and P. F. J. van Velthoven (2002), The budgets of O_3 and CO in the upper troposphere: CARIBIC passenger aircraft results 1997–2001, *J. Geophys. Res.*, *107*(D17), 4337, doi:10.1029/2001JD001529.

Zeng, J., M. Katsumoto, R. Ide, M. Inagaki, H. Mukai, and Y. Fujinuma (2003a), *Data Analysis and Graphic Display System for Atmospheric Research using PC*, *CGER-M014-2003*, pp. 19–77, Cent. for Global Environ. Res., Natl Inst. for Environ. Stud., Tsukuba, Japan.

Zeng, J., Y. Tohjima, Y. Fujinuma, H. Mukai, and M. Katsumoto (2003b), A study of trajectory quality using methane measurements from Hateruma Island, *Atmos. Environ.*, *37*, 1911–1919.

Zhang, X., T. Nakazawa, M. Ishizawa, S. Aoki, S. Nakaoka, S. Sugawara, S. Maksyutov, T. Saeki, and T. Hayasaka (2007), Temporal variations of atmospheric carbon dioxide in the southernmost part of Japan, *Tellus B*, *59*, 654–663.

J. M. Hacker, Airborne Research Australia, Flinders University, P.O. Box 335, Salisbury South, SA 5106, Australia. (jorg.hacker@flinders.edu.au)

G. Inoue, Graduate School of Environmental Studies, Nagoya University, Furo-cho, Chikusa-ku, Nagoya, Aichi 464-8601, Japan. (inouegen@nagoya-u.jp)

R. Saito and T. Yokota, Center for Global Environmental Research, National Institute for Environmental Studies, Onogawa 16-2, Tsukuba, Ibaraki 305-8506, Japan. (saito.ryu@nies.go.jp)